Chapter 5

Satellite-Based Energy Balance Approach to Assess Riparian Water Use

Baburao Kamble, Ayse Irmak, Derrel L. Martin, Kenneth G. Hubbard, Ian Ratcliffe, Gary Hergert, Sunil Narumalani and Robert J. Oglesby

Additional information is available at the end of the chapter

http://dx.doi.org/10.5772/52929

1. Introduction

Previous studies across the High Plains and the Arid West of the United States have produced widely varying impacts of riparian evapotranspiration (ET) on surface and ground water. Many producers as well as various state agencies have advocated removing all trees along the river basins as a method of riparian control for water reclamation. Although eradication of trees might be an effective method for water reclamation in the short-term, it has not been yet proven whether such water savings are possible on a stream level. Mean water use of riparian trees has been reported in relatively few studies, and most of the previous studies have been of short duration. The water use for saltcedar (Tamarix spp.) was estimated at 15.9 L d^{-1} for 10 cm^2 sap wood area (swa) (Smith et al. 1998), 56.8 L d^{-1} for 33 cm^2 swa (Nagler et al. 2003), and 29.9 L d^{-1} for 100 cm^2 swa (Owens and Moore, 2007). The water use for Fremont cottonwood (Populus fremontii S. Wats.) varied from 57.6 L d^{-1} for 33 cm^2 swa (Nagler et al. 2003) to as high as 499.7 L d^{-1} for 833 cm^2 swa (Schaeffer et al. 2000). Riparian plant communities are complex ecosystems that, through an intimate relationship with the fluvial dynamics of river systems, are as much described by their continual cycle of disturbance and succession as by the vegetation that makes up their multi-storied habitats. Currently, there is uncertainty in the water use of riparian systems due to the narrow and sparse vegetation commonly associated with them. Local, state and federal water management regulatory agencies need good quality water use estimates on unmanaged riparian systems. High frequency micrometeorological flux measurements such as Eddy Correlation System (ECS) have been used to estimate water use by balancing fluxes of sensible and latent heat with total energy incident on a riparian area. However, the technique is most effective when

applied to an agricultural land where the plant canopy is relatively homogeneous both in composition and in height, and the fetch is relatively large. Estimating riparian ET in semi-arid river basins is difficult because of the complicated geometry of a typical riparian zone (Goodrich et al., 2000). Riparian forests are typically characterized by long narrow strips of vegetation directly adjacent to stream channels. These strips of forest are often relatively high (~5-20m), not more than 20 m wide on either side of a watercourse and may consist of several different species and size classes of trees (Goodrich et al., 2000). This geometry precludes the use of classical meteorological flux measurements as the required fetch requirements usually are not satisfied. Without the required fetch, the total flux measured using this system will not representf the riparian zone. Water use varies spatially even in the same riparian species because of variation in tree age, height, density, and surroundings. Therefore, the estimation based on in-situ measurements is at stand scale and adds uncertainty when applied to riparian corridors of larger scale. In addition, application of high frequency meteorological flux measurements to quantify ET along stream channels in a basin is limited due to the number of measurement sites needed and the operational expense of such a dense network. The tree sap flow measurements capture variations in transpiration demand as a function of atmospheric demand and water availability. However, there is some uncertainty associated with estimation of stand-level transpiration from individual plant sap flow measurements.

Remote sensing measurements can provide information with a broad spatial coverage and a repeat temporal coverage and avoid the need to rely on field databases. Calculation of water consumption by remote sensing has benefited from significant research efforts over the last 30 years, especially the dedicated energy balance models like the TSEB (Norman et al., 1995), SEBAL (Bastiaanssen, 1998a; 1998b), SEBI (Menenti, 2000), and METRIC^{tm}(Allen et al. 2007b). In this chapter, the method used to estimate ET in riparian areas employs the model known as Mapping Evapotranspiration at high Resolution with Internalized Calibration (METRIC^{tm}) by Allen (2007b). The METRIC^{tm} model (Allen et al. 2007b) requires parameterization of the energy balance and estimates surface energy fluxes based on spectral satellite measurements. The model has auto-calibration capabilities for each satellite image using ground-based calculation of alfalfa reference ET based on hourly weather data. Modifications to the energy balance algorithms for narrow riparian regions that may experience advection and different turbulence characteristics than shorter and more homogeneous surfaces is accomplished by running the METRIC^{tm} model with airborne data collected from June through the end of October 2009 using AISA hyperspectral system hyperspectral system at Center for Advanced Land Management Information's (CALMIT's), onboard Piper Saratoga aircraft. Furthermore, frequent and intensive aerial images help to investigate patterns of surface temperature at various spacings inside riparian structures and the variation with wind speed and wind direction. This data is also used to understand the partitioning of the available energy between understory and overstory in the riparian system. There is some uncertainty in estimating ET from riparian systems with SRS based energy balance due to the narrow and sparse vegetation commonly associated with them. However, the high resolution of Landsat images is extremely useful for assessing ET patterns and might be the most suit-

http://dx.doi.org/10.5772/52929

able method (Irmak and Kamble, 2009;, Kamble and Irmak, 2011;2008; Irmak et al., 2011). The literature also shows that the thermal signatures of the riparian systems indicate a pretty complete picture of the amount of evaporative cooling within boundaries of the ecosystem, including evaporation from wet soil or under structure. Therefore, the METRIC^{tm} or related remote sensing based energy balance approach is one of the better means to make the ET estimates and to monitor before and after vegetation and land-use modification.

The information presented here is taken from the results of projects conducted at the University of Nebraska. Our primary goal in this chapter is to illustrate spatiotemporal estimation of ET using satellite-and aerial derived spectral radiances in conjunction with a land surface energy balance model and flux measurements to evaluate water use and water distribution within and between riparian systems, including invasive species, along the North Platte River Basin (NPRB) in Nebraska (NE). Specific objectives were to quantify daily and seasonal distributions of ET in riparian systems within the NPRB, quantify surface energy balance flux components for riparian systems, and compare water use among riparian species, both native and invasive, by utilizing ET maps together with riparian species distribution map.

2. Material and methods

2.1. Study area

The Nebraska Panhandle is an area in western Nebraska bounded by the mountainous (Rocky Mountains) states of Wyoming and Colorado on the west and the city of North Platte,Nebraska on the east, wherein the main stem of the North Platte River flows from west to east. The Nebraska panhandle roughly encompasses the area in Nebraska between 102° and 104°W longitude and 41° and 43°N latitude. The elevation ranges from 3,000-5,000 ft and the growing season is characterized by hot days and cool nights. The Panhandle additionally has a high desert-type semi-arid climate receiving 14-16 inches rainfall per year. Flows in the North Platte River are derived mainly from snowmelt runoff from the Rocky Mountains and surface runoff and ground-water discharge (Bentall and Shaffer, 1979; Gutentag et. al., 1984). The eastern and central parts of Nebraska predominantly are cultivated-agricultural land with increasing amounts of rangeland to the west (Center for Advanced Land Management Information Technologies, 2000; U.S. Geological Survey, 1999-2000). Riparian vegetation is restricted to lowlands located along the North Platte River and its tributaries. Forests and grasslands (including wet meadows) in the riparian zone are the predominant communities, but other categories are present including herbaceous, shrub, and emergent wetlands (Currier et. al., 1985).

2.2. Satellite image processing

A total of 8 Landsat5 and Landsat7 satellite images (Path 33, Row 31) from 2005 were used for this study (table 2). Each Landsat scene size is approximately 170 km X 185 km with a

repeat cycle of 16 days. The Thematic Mapper (TM) sensor on-board Landsat 5 has seven spectral bands with 30 m spatial resolution in reflective bands and 120 m resolution in thermal bands. The Enhanced Thematic Mapper (ETM) on-board Landsat 7 has eight spectral bands including panchromatic band (not used in this study). UTM zone 13 and NAD 1983 was the projection and datum used. For Landsat 7 imagery, the high gain on the thermal band was used. The Landsat 7 thermal band is acquired in both low and high gain. The low gain provides an expanded dynamic range generating less saturation at high values, but lower radiometric resolution (sensitivity).

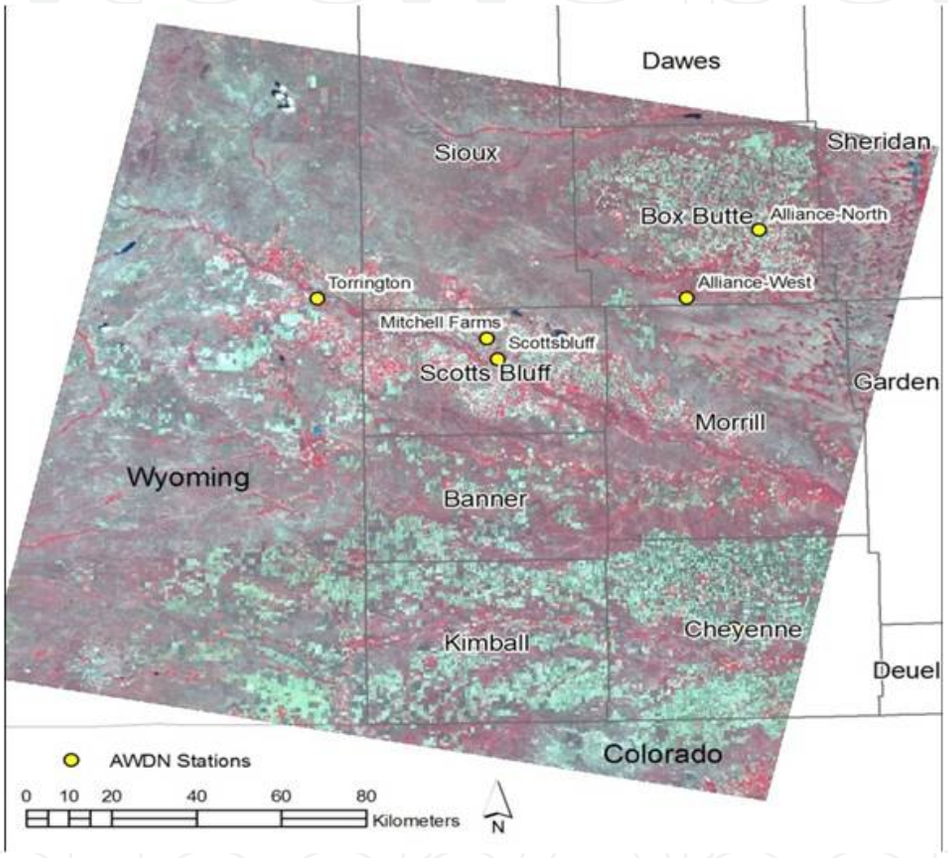

Figure 1. Geographic footprint of Landsat path 33, row 31. Images cover parts of the Nebraska Panhandle, Wyoming, and Colorado.

The thermal high gain band has higher radiometric resolution but provides a less dynamic range.The spatial resolution of ETM in reflective bands is 30 m and 60 m in the thermal bands. Landsat7 ETM images have missing data in the form of a wedge due to failure of Scan Line Corrector (SLC) on May 31, 2003 referred to as SLC off images. Processing of SLC-off images requires replacing the missing data. Gap filling was used utilizing same time images with spectral information taken from the neighbouring pixels. The convolution filtering algorithm with majority function was used to replace the missing data. The METRIC^{tm} model (Allen et al. 2007b) estimated energy fluxes using the remotely sensed data as input (A general overview of the METRIC^{tm} model is presented in the next section). The model maker

http://dx.doi.org/10.5772/52929

tool of Erdas Imagine® image processing software (Leica Geosystems Geospatial Imaging, LLC) was used to code the METRIC^{tm} algorithms. An iterative procedure was followed for sensible heat flux estimation using hot and cold pixels. From each processed image, average of 9 (3 X 3) pixels cantered over the field measurement location was used for the comparison of model estimated fluxes with the field measurements.

2.3. Meteorological data

High quality hourly weather data consisting of air temperature, relative humidity, wind speed, incoming solar radiation, and precipitation are required for the operation of the METRIC^{tm} model. Hourly weather data were acquired from the High Plains Regional Climate Center's (HPRCC) Automated Weather Data Network (AWDN). Weather data were acquired for 2005 from the Scottsbluff (latitude: 41.22 N; longitude: 103.02 W; elevation=1208 m) AWDN station to calibrate METRIC^{tm} model. The weather data was quality controlled following the recommendations of Allen et al., 1996; 1998; 2005 and by ASCE-EWRI (2005) for all the weather stations in and out of Landsat path. Table 2 shows the list of AWDN stations used in this analysis. Hourly and daily observed solar radiation (R_s) values were compared with that of calculated clear sky solar radiation (R_{so}).

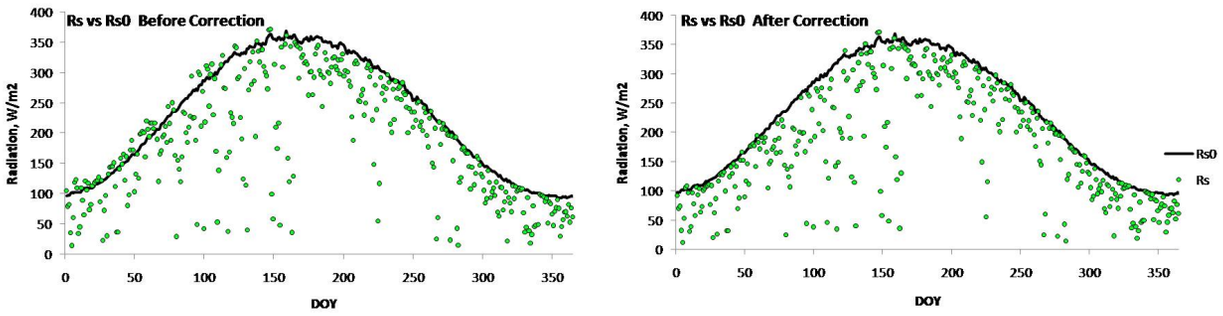

Figure 2. Scottsbluff 2005 corrected observed solar radiation (W/m^2) and calculated clear sky solar radiation (W/m^2). For DOY 1-123 (03 May) a 6% decrease in Rs values were applied.

R_{so} is the theoretical estimate of incoming solar radiation to the ground surface on a clear sky day with low atmospheric aerosol content (e.g. no haze, dust, smoke from fires, etc.) and is calculated based on atmospheric pressure, sun angle, and precipitable water in the atmosphere (i.e. figure 2). Corrections are only applied when the data exhibits systematic errors eg. R eg. Rs>Rso. Individual values are corrected. Reasons for errors in the solar radiation values can be due to misalignment or a nonrepresentative calibration of the sensor. reference evapotranspiration (ETr) values were calculated using the ASCE-EWRI (2005) standardized Penman-Monteith equation for alfalfa reference. These calculations were carried out using Ref-ET software (University of Idaho and Allen, 2003

Station	Latitude	Longitude	Elevation (m)
Alliance-North, NE	42.18	102.92	3980.10
Alliance-West, NE	42.02	103.13	3980.00
Arapahoe Prairie, NE	41.48	101.85	3600.00
Arthur, NE	41.65	101.52	3598.08
Gordon, NE	42.73	102.17	3638.45
Gudmundsen, NE	42.07	101.43	3441.60
Mitchell Farms, NE	41.93	103.70	3602.36
Scottsbluff, NE	41.88	103.67	3963.25
Sidney, NE	41.22	103.02	4320.87
Sterling, CO	40.47	103.02	3937.01
Torrington, WY	42.03	104.18	3989.50

Table 1. Lists of observation stations for calibration and validation

Figure 3 shows the riparian species as documented by the AISA system onboard CALMIT's Piper Saratoga aircraft on NE Panhandle. This map was integrated with seasonal ET maps obtained with METRIC^{tm} model. Hyperspectral remote sensing holds great promise for research on invasive species. Spectral information provided by hyperspectral sensors on AISA system can detect invaders at the species level across a range of community and ecosystem types. This gigh resolution classification provides a valuable description of spatial variation in riparian, serves as a baseline to measure ET in riparian, and is essential for prioritizing riparian restoration treatments in the basin.

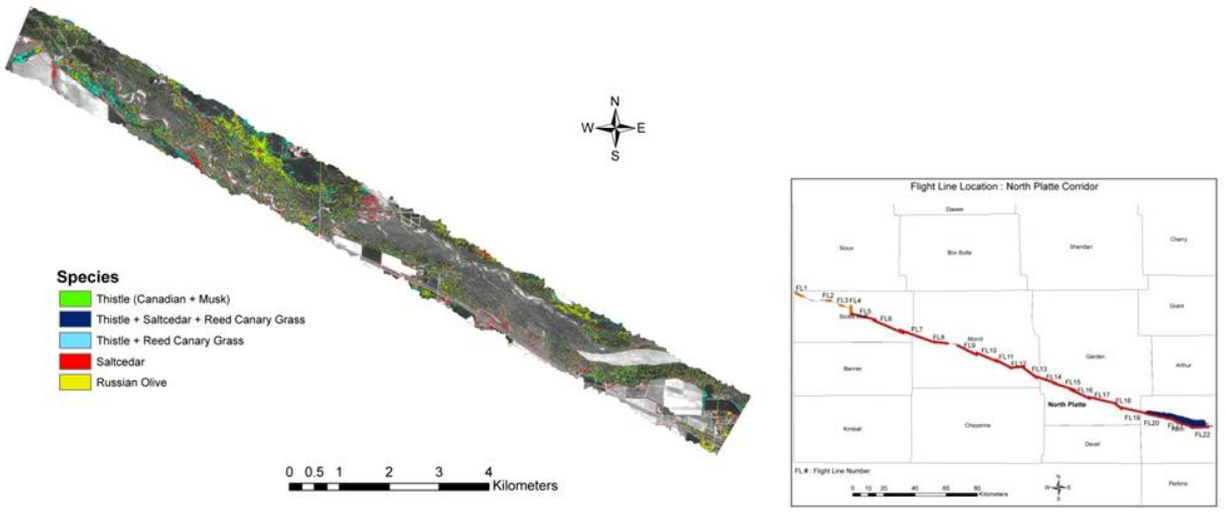

Figure 3. Invasive species distribution in 2005 for flight line #3 on Path 33, Row 31.

http://dx.doi.org/10.5772/52929

2.4. Land surface energy balance model

The landsat images for 2005 for Path32 Row 31 were processed using the algorithms in the METRIC^{tm} (2007a; 200b) model which requires parameterization of the energy balance and estimation of surface energy fluxes based on spectral satellite measurements (Allen et al., 2007). The model is originated from the SEBAL model and a "hybrid" energy balance model that uses thermal bands from Landsat imagery to compute ET. In particularly, it combines remotely-sensed energy balance (satellite) data and ground-based ETr (reference ET) data to determine ET. METRIC^{tm} computes LE as a residual of the energy balance as:

$$LE = R_n - G - H \tag{1}$$

where R_n is the net radiation, G is the soil heat flux, H is the sensible heat flux, and LE is the latent heat flux. The units for all the fluxes are in W m^{-2}. METRIC^{tm} calculates net radiation (R_n) as the difference between incoming radiation at all wavelengths and reflected short-wavelength (~ 0.3 – 3 μm) and both reflected and emitted long-wavelength (3~60 - μm) radiation (Allen et al., 2007a). The LE time integration was split into two steps. The first step was to convert the instantaneous value of LE into daily values of actual ET (ET_{24}) values by holding the reference ET fraction constant (Allen et al., 2007b). An instantaneous value of ET (ET_{inst}) in equivalent evaporation depth is the ratio of LE to the latent heat of vaporization. usually range from 0 to 1.05 and is defined as the ratio of instantaneous ET (ET_{inst}) for each pixel to the alfalfa-reference ET calculated using the standardized ASCE Penman-Monteith equation for alfalfa (ET_r) following the procedures given in ASCE-EWRI (2005):

$$\text{ETrF} = \frac{\text{ET}_{\text{inst}}}{\text{ET}_{\text{r}}} \tag{2}$$

The procedures outlined in ASCE-EWRI (2005) were used to calculate parameters in the hourly ET_r equation. The daily ET at each pixel was estimated by consideringETrF and 24 hour ET_r as:

$$\text{ET}_{24} = \text{ET}_{\text{r}}\text{F} \times \text{ET}_{\text{r}-24} \tag{3}$$

where ET_{24} is the daily value of actual ET (mm day^{-1}), $ET_{r\text{-}24}$ is 24 hour ET_r for the day of image and calculated by summing hourly ET_r values over the day of image. In order to produce monthly and seasonal ET maps, individual ET_rF maps from each image in the analysis were generated from METRIC and interpolated using a cubic spline model. The spline model is deterministic interpolation method which fits a mathematical function through data points to create a surface (Hartkamp, 1999). The spline surface was achieved through weights (λ_i) and number of points (N). A regularized spline was used because this method

results in a smoother surface. Daily images were generated by interpolation used for monthly and seasonal ET calculation.

3. Result and discussion

A daily soil water balance model was applied for 2005 using precipitation and ETr from the for all weather stations (Table1). The water balance model estimates residual evaporation from bare soil for each of the Landsat image dates. The model is based on the two-stage daily soil evaporation model of the United Nations Food and Agriculture Organization's Irrigation and Drainage Paper 56 (Allen et al., 1998). The soil water balance is set up assuming a loam soil having a water content at field capacity and the wilting point of 0.3 cm^3/ cm^3 and 0.15 cm^3/ cm^3, respectively and having 10 mm of readily evaporable water in the upper 12.5 cm of soil. Figure 4 shows a simulation of evaporation from bare soil. The results from the soil water balance were used to determine reference evapotranspiration fraction (EtrF) for hot pixel selection, an internal calibration step for running METRIC^{tm}.

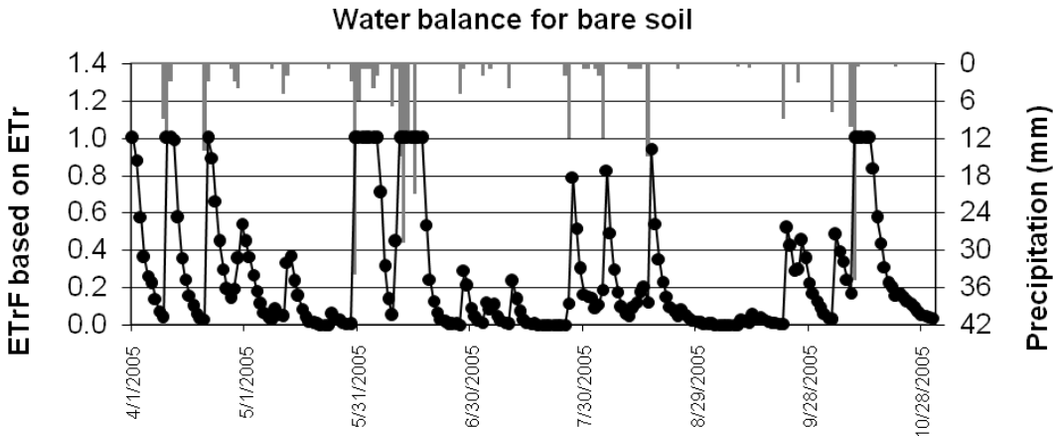

Figure 4. Soil water balance for bare soil calculated from meteorological data from Scottsbluff, NE 2005.

An example of soil water balance simulations for the top 0.125 meter of soil based on soil properties and meteorological data from the Scottsbluff, NE AWDN station is shown in Figure 4. It should be noted, that the soil water balance indicates that the residual evaporation from bare soil on 10/14/2005 corresponds to an ET_rF of 1.0 as a result of relatively large amounts of precipitation a few days prior to the image date. An ET_rF value for the hot pixel of this magnitude leaves a very small margin up to the ET_rF of 1.05 generally assigned to the cold pixel. For reasons discussed under the individual images below, the ET_rF for the hot pixel has been assigned the value 0.8 for this image.

We utilized both satellite and air-bone remote sensing data with an energy balance model to provide a better understanding and quantification of evapotrabspiration for selected invasive species. We utilized METRIC^{tm} to quantify spatial distribution and seasonal variation of actual ET over riparian zone in North Platte River during growing season for 2005. Next, we

http://dx.doi.org/10.5772/52929

integrated ET maps with invasive species map to estimate the mean and the range of water use for each riparian species. The invasive species map developed using hyperspectral aerial imagery (AISA) in 2005 at 1.5 meter resolution for the North Platte River Basin was used. The measured components of the water balance (precipitation and ETrF based on ETr) from Scottsbluff, NE were evaluated to determine ETrF for the hot pixel selection and to determine the net ground-water recharge that occurred during the study. Precipitation and ETrF were the dominant components of the water balance with ground-water storage being a comparatively minor term. The ETrF is highly variable over the landscape because of the variability in landuse, climate, soil properties, and management practices. Soil properties affect surface soil evaporation and energy balances, including soil heat flux and sensible flux; causing within-field and across field variability in ETrF. Much of this variability occurs at the field scale, making it nearly impossible to quantify ET spatially using more traditional and conventional methods. Figure 6 shows monthly ETrF for path 33, row 31 in 2005. The spline model requires two images each in the preceding and subsequent months for the month to be interpolated. Because only one image was available for the month of April, a new ETrF image was created for April 23rd from MODIS 250m NDVI data. The methods used were the same as the cloud filling method using MODIS 250m NDVI data.

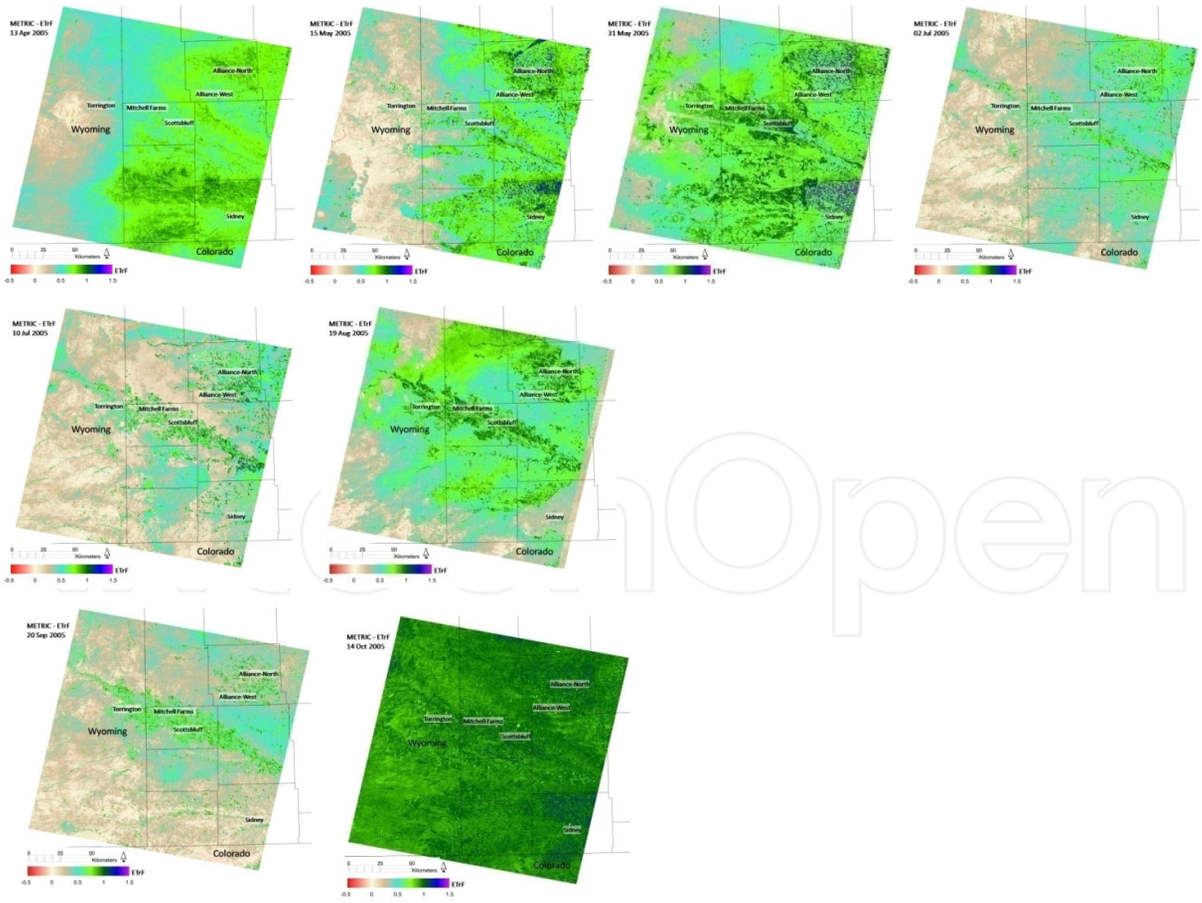

Figure 5. Calculated ETrF (reference ET faction) for individual Landsat dates in 2005 path 33, row 31.

Figure 6 shows the expected progression of ETrF during a growing season as surface conditions changed. The spatial distribution of daily ETrF estimations using the Landsat overpass on May 31, 2005 and August 19 2005 were highly variable ranging from 0.6 mm day^{-1} to as high as 0.9 mm day^{-1} across the images. Most of the variability was due to differences in land use and riparian species. The land use in the top part of the study area is mainly agricultural land that is devoid of standing crops in early May. The bottom part of the study area is mostly grazed rangeland or natural vegetation dominated by green vegetation in early spring, resulting in higher ET.

Monthly ET maps were summed to obtain total seasonal ET for the study area. Figure 6 shows the progression of ET from May through September in 2007 across the Panhandle derived using spline interpolation algorithm. The monthly ET maps generated by the METRICtm model showed a good progression of ET during the growing season as surface conditions continuously changed. Results showed that salt cedar water use was lowest compared to other invasive species. Russian olive also has substantial water use during growing season. For most species seasonal actual ET ranged from 20 to 35 inches. From figure 2 of hyperspectral image of invasive species distribution and figure 6 of monthly ET maps produced with METRICtm for Landsat path 33 row 31 in 2005 we have an indication of the water use during the growing season for individual invasive species. Comparison is difficult due to non-uniform distribution of species and differences in age. Water use varied considerable even in the same species due to plant density, plant distribution and plant height of individual species. ET roughly ranged from 12 in to as high as 43 in for all the invasive species for May 1st to September 31st. Average actual seasonal ET ranged from 27 inches to 30 inches for all the invasive species. Overall, the remote sensing based energy balance approach based on landsat image in conjunction with high resolution hyperspectral image was useful to obtain distribution of ET estimates from riparian systems.

The ET was lower early in the growing season and gradually increased as the riparian species increasingly transpire water towards the mid season. The METRIC^{tm} model was also able to estimate the decreasing evaporative losses towards the end of the season and after the harvest. However, in figures 6 subfigures July, August and September show visible distinctions in ET among the riparian species. To calculate species wise distribution one needs full knowledge of the study area land use with hyperspectral imagery classification. Since requirement of accurate riparian species type identification can increase costs of ET mapping at larger scales, this is an advantage of METRIC^{tm} because the model does not require information on soil and management practices.

July is usually the peak ET month with high incoming solar radiation, high temperatures, and large vapor pressure deficit all contributing to increased ET. The ET shows variation throughout the district as a function of different ET rates of various land covers, including riperian species, agriculture crops and natural vegetation, etc. With physiological maturity, leaf aging and senescence, ET starts to decrease gradually in September. At the start of fall, leaves of plants start falling in October, most of the ET in this month represents the soil evaporation component of ET. As shown in monthly ET maps, mapping ET on large scales can provide vital information on the progression of ET for various vegetation surfaces over

http://dx.doi.org/10.5772/52929

time. Information gained enables the prediction of the timing and the spatial extent of potential depletions or gains in both the short-term and in the long-term management of surface and ground water.

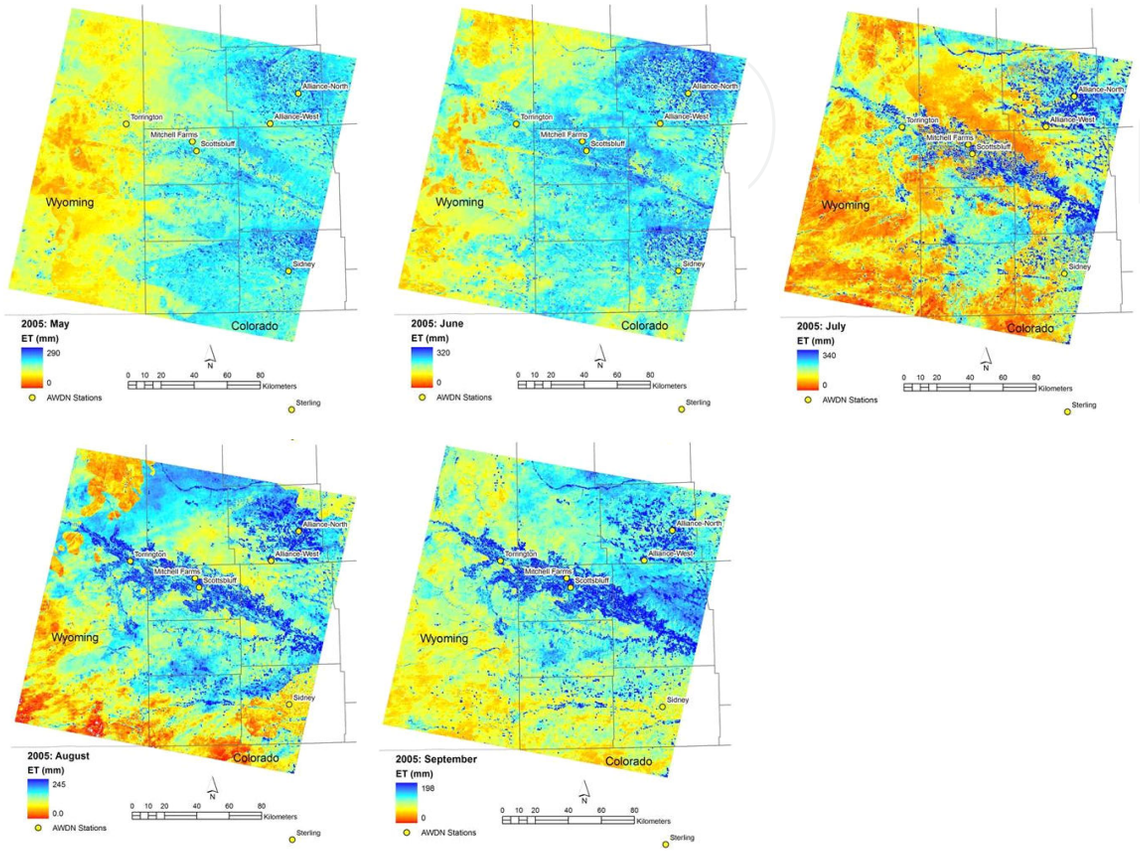

Figure 6. Monthly ET (mm) maps produced with METRIC^{tm} for Path 33 Row 31 in 2005.

The seasonal ET (mm) maps generated by the METRIC^{tm} model showed spatial and temporal distribution of relative ET during the 2005 season as land surface conditions continuously changed (Figure. 8). The information also allowed us to follow the seasonal trend in ET for major land use classes on the image. Water consumption by the riperian species is higher than the water consuption for other landuse in the Panhandle.

The frequency distribution and the basic statistics for seasonal ET including all species are presented in Figure 8 and and summarized in Table 2, respectively. Statistics provided in Table 2 are for the water use during the growing season for individual invasive species. Comparison is difficult due to the non-uniform distribution of species and difference in age. Water use varied considerable even in the same species due to plant density, plant distribution and plant height of individual species. ET roughly ranged from 12in to as high as 43 in for all the invasive species for May 1st to September 31st. Average actual seasonal ET ranged from 27 inches to 30 inches for all the invasive species.

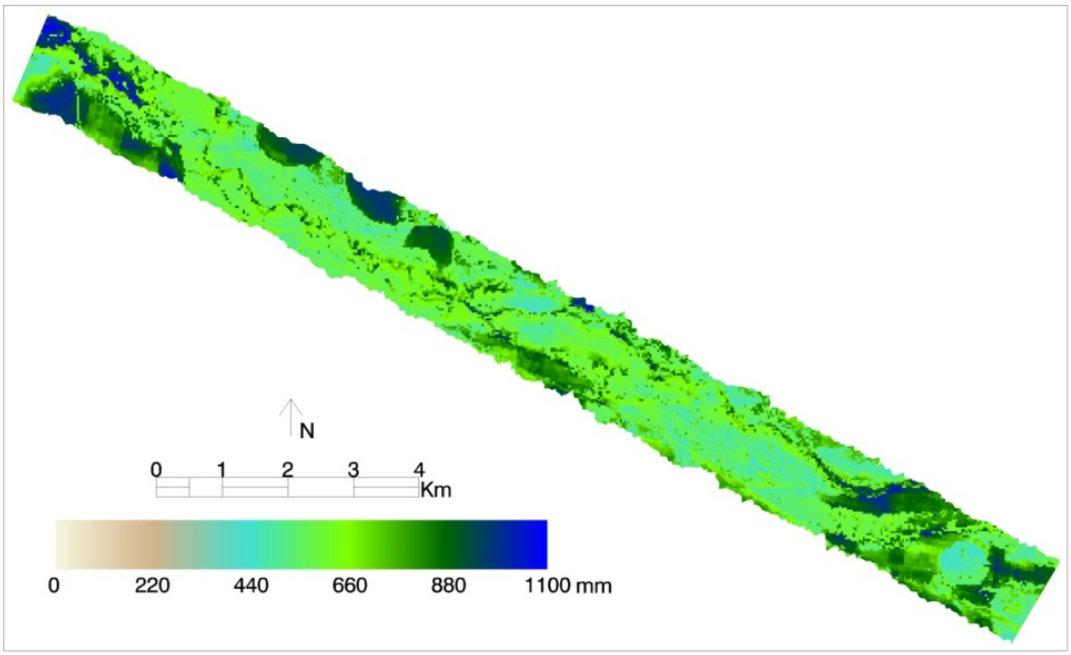

Figure 7. Seasonal ET (mm) map from May 01 through September 30 in 2005 for Path 33 Row 31.

Species	Minimum	Maximum	Average
Russian Olive	12	42	29
Salt Cedar	14	40	27
Thistle	12	42	30
Thistle+Salt Cedar+Reed Canary Grass	15	41	28
Thistle+Reed Canary Grass	16	43	30

Table 2. Comparison of seasonal water use in inches from May 1st to September 30th in 2005.

Figure 8 shows the histogram of seasonal actual ET for individual and combination of various riparian species. The y axis on the figure (histogram) shows the number of AISA pixels (1.5 m) for each riparian species while x axis shows corresponding actual ET values in inches. We observed that there is no single ET value for invasive species. Results showed that salt cedar water use was lowest compared to other invasive species. Russian olive also has substantial water use during growing season. For most species seasonal actual ET ranged from 20 to 35 inches. Overall, the remote sensing based energy balance approach based on the landsat image in conjunction with high resolution hyperspectral image was useful to obtain distribution of ET estimates from riparian systems.

http://dx.doi.org/10.5772/52929

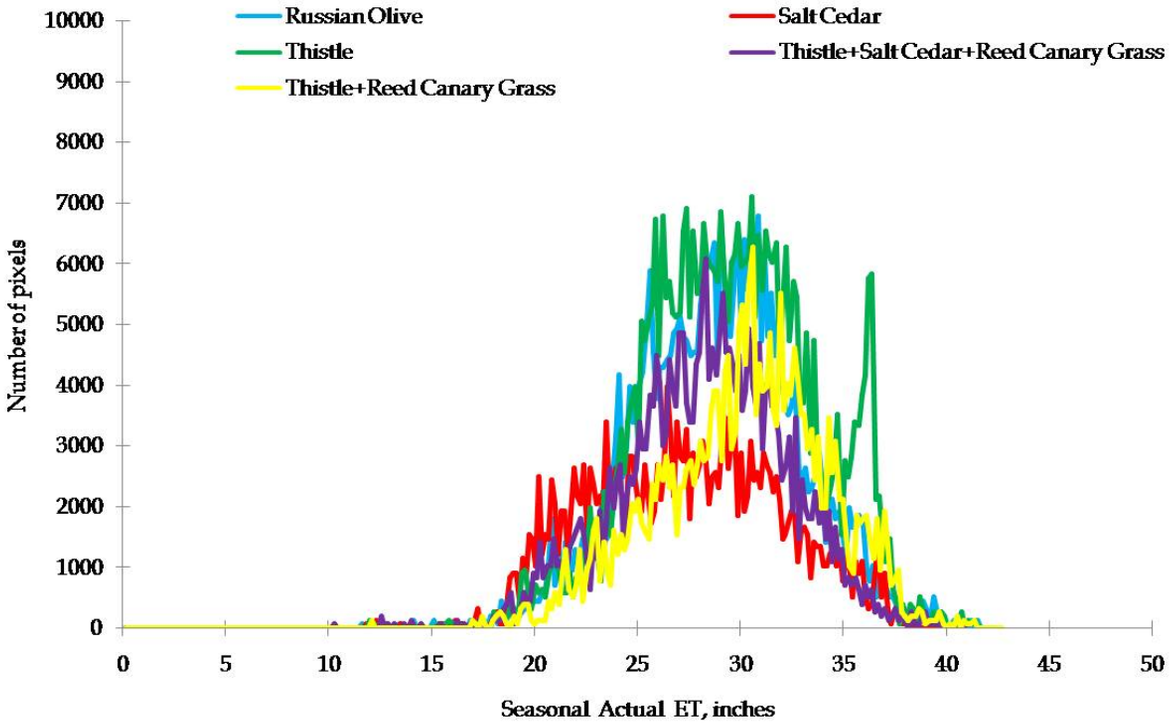

Figure 8. The comparison of water use (seasonal actual ET, inch) for individual and combination of various riparian species.

4. Conclusion

This study focused on the use of multi-temporal landsat data and hyperspectral remote sensing data to calculate daily and seasonal actual ET based upon satellite energy balance model such as METRIC^{tm}. The remotely sensed measurements using METRIC^{tm}.provide the estimation of spatial distribution of instantaneous ET, which can be integrated into daily and seasonal ET values. The seasonal spatial distribution maps help to explain the water consumption for the di ▪ erent riperean species season. Based on maps we have developed guidelines on riparian water use which will be of benefit to the state, particularly with regard to riparian control for water acclamation. Satellite-based measurements can provide such information and avoid the need to rely on field databases. The ET values for a given species varies due to the density and age of the plant species. By integrating the hyperspectral images with the METRIC™ model, we obtain the following seasonal ET values (May 1 through September 1, 2005) for the following invasive species: Salt Cedar (Tamarisk) 26.8 inches (680 mm) or 2.23 acre-feet water, Russian Olive 26.7 inches (677 mm) or 2.23 acre-feet water, average Canada and Musk Thistle 27.9 inches (708 mm). Using developed figures, this vegetation transpires approximately 30,453 acre-feet of water per season. Since willows, cottonwood trees and some grasses transpire approximately the same amount of water, revegetation with these species would result in a net “no gain” of water conservation. Based

on the analysis of images from AISA and Landsat, we show that ET varies even in the same species (i.e. salt cedar) because of variation in tree age, height, density, and surrounding area. Nevertheless, further studies are necessary to expand this method in conjuction with hyperspectral data to obtain species wise water use distribution. The METRIC^{tm} model should be tested for its suitability for other climate conditions found in Nebraska and an assessment made of the spatial variability of the calibration parameters is needed.

Acknowledgements

The. authors thank to the University of Nebraska Foundation, Anna H. Elliot Fund grants which supported this work and University of Idaho for METRICtm modeling support.

Author details

Baburao Kamble, Ayse Irmak, Derrel L. Martin, Kenneth G. Hubbard, Ian Ratcliffe, Gary Hergert, Sunil Narumalani and Robert J. Oglesby

University of Nebraska-Lincoln (UNL), Lincoln, USA

References

[1] Allen, R. G. (1996). Assessing Integrity of Weather Data for Use in Reference Evapotranspiration Estimation. J. Irrig. Drain. Eng ASCE, , 122, 97-106.

[2] Allen, R. G., Pereira, L., Raes, D., & Smith, M. (1998). Crop Evapotranspiration, Food and Agriculture Organization of the United Nations, Rome, It. 925-1-04219-530-0p.

[3] Allen, R. G., Tasumi, M., & Trezza, R. (2007a). Satellite-based energy balance for mapping evapotranspiration with internalized calibration (METRIC)- Model. ASCE J. Irrigation and Drainage Engineering , 133(4), 380-394.

[4] Allen, R. G., Tasumi, M., Morse, A. T., Trezza, R., Kramber, W., Lorite, I., & Robison, C. W. (2007b). Satellite-based energy balance for mapping evapotranspiration with internalized calibration (METRIC)- Applications. ASCE J. Irrigation and Drainage Engineering , 133(4), 395-406.

[5] -E, A. S. C. E., & , W. R. I. (2005). The ASCE Standardized reference evapotranspiration equation. ASCE-EWRI Standardization of Reference Evapotranspiration Task Comm. Report, ASCE Bookstore, 078440805pages.(40805)

[6] Bastiaanssen, W. G. M., Menenti, M., Feddes, R. A., & Holtslag, A. A. M. (1998a). A remote sensing surface energy balance algortithm for land (SEBAL). Part 1: Formulation. J. of Hydrology , 198-212.

[7] Bastiaanssen, W. G. M., Pelgrum, H., Wang, J., Moreno, Y. J. F., Roerink, G. J., Roebeling, R. A., & van der Wal, T. (1998b). A remote sensing surface energy balance algortithm for land (SEBAL). Part 2: Validation. J. of Hydrology 212-213: 213-229.

[8] Bentall, Ray., & Shaffer, F. B. (1979). Availability and use of water in Nebraska, 1975: Conservation and Survey Division, University of Nebraska-Lincoln, Nebraska Water Survey Paper 48, 121 p.

[9] Center for Advanced Land Management Information Technologies (CALMIT), 2000, Delineation of 1997 land use patterns for the Cooperative Hydrology Study in the central Platte River Basin: Lincoln, Nebraska, CALMIT, 73 p., accessed August 29, 2008, at http://www.calmit.unl.edu/cohyst/data/1997_finalreport.pdf

[10] Currier, P. J., Lingle, G. R., & Van Derwalker, J. G. (1985). Migratory bird habitat on the Platte and North Platte Rivers in Nebraska: Grand Island, Nebr., Platte River Whooping Crane Maintenance Trust, 177 p.

[11] Goodrich, D. C., Scott, R., Qi, J., Goff, B., Unkrich, C. L., Moran, M. S., Williams, D., Schaeffer, S., Snyder, K., Mac, R., Nish, T., Maddock, D., Pool, A., Chehbouni, D. I., Cooper, W. E., Eichinger, W. J., Shuttleworth, Y., Kerr, R., & Marsett, W. N. (2000). Seasonal estimates of riparian evapotranspiration using remote and in situ measurements: Agricultural and Forest Meteorology, , 105(1-3), 281-309.

[12] Gowda, P. H., Chávez, J. L., Colaizzi, P. D., Evett, S. R., Howell, T. A., & Tolk, J. A. (2008). ET mapping for agricultural water management: present status and challenges. Irrig. Sci. , 26, 223-237.

[13] Gutentag, E. D., Heimes, F. J., Krothe, N. C., Luckey, R. R., & Weeks, J. B. (1984). Geohydrology of the High Plains aquifer in parts of Colorado, Kansas, Nebraska, New Mexico, Oklahoma, South Dakota, Texas, and Wyoming: U.S. Geological Survey Professional Paper 1400B, 63 p.

[14] Hartkamp, A. D., De Beurs, K., Stein, A., & White, J. W. (1999). Interpolation Techniques for Climate Variables, NRG-GIS Series 9901CIMMYT: Mexico, DF, http://www.cimmyt.org/Research/nrg/pdf/NRGGIS%2099pdf [1 Sep 2004].

[15] High Plains Regional Climate Center,(2006). National Weather Service surface observations and automated weather data network data: Lincoln, Nebraska, University of Nebraska, digital data, accessed November 1, 2006, at http://www.hprcc.unl.edu/.

[16] Irmak, A., & Kamble, B. (2009). Evapotranspiration Data Assimilation with Genetic Algorithms and SWAP Model for On-demand Irrigation. Irrigation Science. 28:101-112 (DOIs00271-009-01939).

[17] Irmak, A., Ratcliffe, I., Ranade, P., Hubbard, K. G., Singh, R. K., Kamble, B., Allen, R. G., & Kjaersgaard, J. (2010). Estimation of land surface evapotranspiration: A Satellite Remote Sensing Procedure. Great Plains Research. 21(1):April 2011.

[18] Irmak, A., Rundquist, D., , S., Narumalani, G., Hergert, , & Stone, G. (2009). Satellite-Based Energy Balance to Assess Riparian Water Use. UNL. Lincoln, NE. USGS 104b final report. 11 p.

[19] Irmak, A., Ratcliffe, I., Ranade, P., Irmak, S., Allen, R. G., Kjaersgaard, J., Kamble, B., Choragudi, R., Hubbard, K. G., Singh, R., Mutiibwa, D., & Healey, N. (2010). Seasonal Evapotranspiration Mapping Using Landsat Visible and Thermal Data with an Energy Balance Approach in Central Nebraska. Remote Sensing and Hydrology. Special Issue IAHS Publ. 3XX, 2011

[20] Irmak, S., Howell, T. A., Allen, R. G., Payero, J. O., & Martin, D. L. (2005). Standardized ASCE Penman-Monteith: impact of sum-of-hourly vs. 24-hour time step computations at reference weather station sites. Trans. ASABE. 48

[21] Kamble, B., & Irmak, A. (2011). Remotely Sensed Evapotranspiration Data Assimilation for Crop Growth Modeling, Evapotranspiration, Leszek Labedzki (Ed.), 978-9-53307-251-7InTech.

[22] Kamble, B., & Irmak, A. (2008). Assimilating Remote Sensing-Based ET into SWAP Model for Improved Estimation of Hydrological Predictions," Geoscience and Remote Sensing Symposium, 2008. IGARSS 2008. IEEE International, no., pp.III-1036-III-1039, 7-11 July 2008 (DOI:10.1109/IGARSS.2008.4779530), 3

[23] Kjaersagaard, J., & Allen, R. G. (2010). Remote Sensing Technology to Produce Consumptive Water Use Maps for the Nebraska Panhandle. Final completion report submitted to the University of Nebraska. 60 pages.

[24] Landon, M. K., Rus, D. L., Dietsch, B. J., Johnson, M. R., & Eggemeyer, K. D. (2009). Evapotranspiration rates of riparian forests, Platte River, Nebraska, 2002-06: United States Geological Survey Scientific Investigations Report p., 2008-5228.

[25] Menenti, M. (2000). Evaporation. In: Schultz GA, Engman ET (eds.). Remote sensing in hydrology and water management. Springer Verlag, Berlin Heidelberg New York, , 157-188.

[26] Nagler, P. L., Glenn, E., & Thompson, T. L. (2003). Comparison of transpiration rates among saltcedar, cottonwood and willow trees by sap flow and canopy temperature models. Agricultural and Forest Meteorology , 116, 73-89.

[27] Norman, J. M., Divakarla, M., & Goel, N. S. (1995). Algorithms for extracting information from remote thermal-IR observations of the Earth's Surface. Remote Sensing of Environment, , 51, 157-168.

[28] Owens, K. M., & Moore, G. W. (2007). Saltcedar water use: realistic and unrealistic expectations. Range. Ecol. & Manage. , 60, 553-557.

[29] Ranade, P. (2010). Spatial Water Balance for Bare Soil. University of Nebraska. Report, 10 pp.

[30] Schaeffer, S. M., Williams, D. G., & Goodrich, D. C. (2000). Transpiration of cottonwood/willow forest estimated from sap flux. Agricultural and Forest Meteorology 105(1-3):257-270.

[31] Singh, R. K., Irmak, A., Irmak, S., & Martin, D. L. (2008). Application of SEBAL Model for Mapping Evapotranspiration and Estimating Surface Energy Fluxes in South-Central Nebraska. J. Irrigation and Drainage Engineering , 134(3), 273-285.

[32] Smith, S. D., Devitt, D. A., Sala, A., Cleverly, J. R., & Busch, D. E. (1998). Water relations of riparian plants from warm desert regions. Wetlands , 18, 687-696.

IntechOpen